

Supplementary Material S1 - Mn K edge Second Derivative Shapes

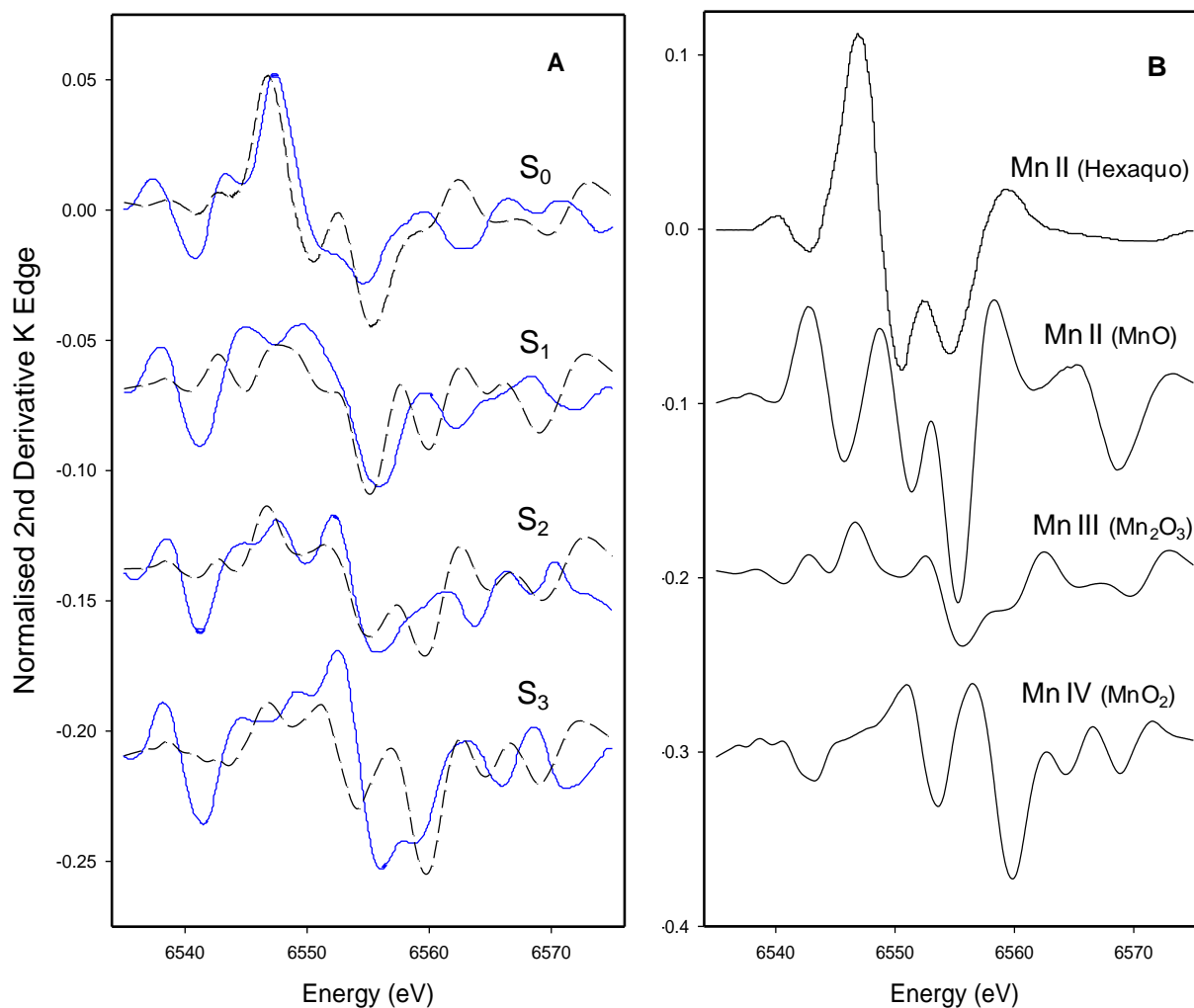


Fig S1 A: Plots of the second derivative spectra of normalized K edge absorption energy profiles for the deconvoluted S states (reproduced from Dau et al. [13a]) (—), together with synthesized second derivative plots formed from combinations of the pure compound spectra in S1 B (---). Combinations are; S_0 ($\text{Mn}^{\text{II}}(\text{Hexaquo})_{0.25}, \text{Mn}^{\text{III}}_{0.75}$), S_1 ($\text{Mn}^{\text{II}}(\text{MnO})_{0.25}, \text{Mn}^{\text{III}}_{0.5}, \text{Mn}^{\text{IV}}_{0.25}$), S_2 ($\text{Mn}^{\text{III}}_{0.75}, \text{Mn}^{\text{IV}}_{0.25}$), S_3 ($\text{Mn}^{\text{III}}_{0.5}, \text{Mn}^{\text{IV}}_{0.5}$). Plots are progressively vertically offset from the S_0 position.

B: Second derivative spectra of normalized K edge absorption energy profiles for several pure Mn-oxy species of defined Mn oxidation state (reproduced from Dau et al. [13a]). Progressively offset as in A

Supplementary Material S2 – S State $K\beta_{1,3}$ Spectra

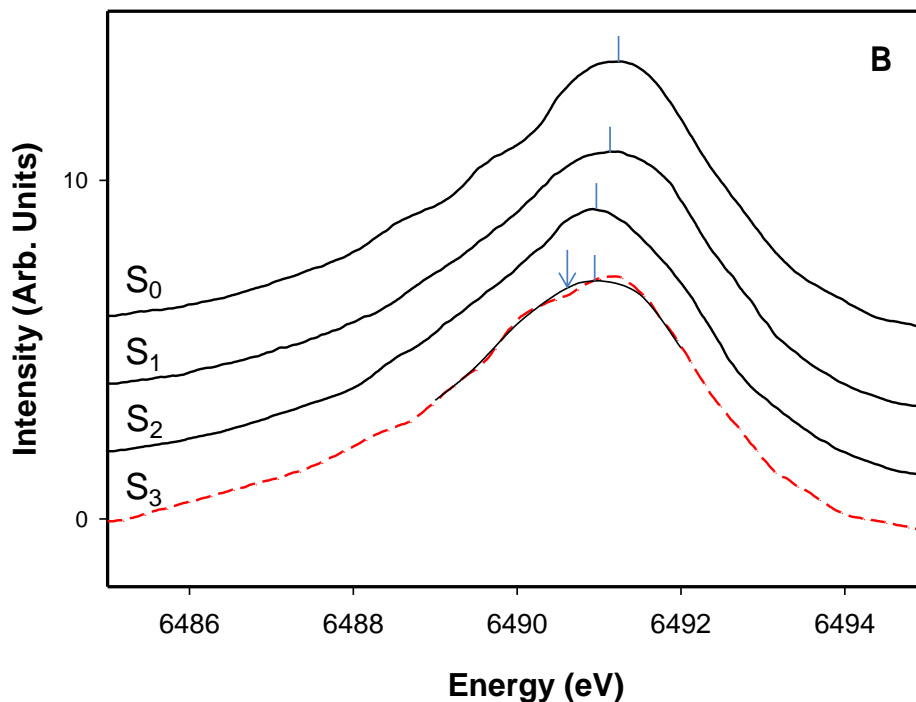


Fig S2: Reproduced Mn $K\beta_{1,3}$ fluorescence spectra for the de-convoluted S states of PS II, from Messinger et al. [12b]. Indicated with bars are our estimates of the peak E_0 positions and the local polynomial smoothing used to estimate the E_0 position for S_3 (solid curve). Also shown on the S_3 trace (arrow) is the expected peak position for a pure Mn^{IV} oxidation level, from the calibration line of Visser et al. in Fig 5, main text

Supplementary Material S3 – Absorption Edge Region Profiles

As stated earlier, a full ab initio computational simulation of the Mn K edge shape of the OEC is formidable, but certain key features relevant to the discussions here may be readily examined in a simplified heuristic manner (ie. in the spirit of our earlier TDDFT examination of XANES, ref [14] Supplementary Material S8). Dau et al have previously used qualitative/semi-quantitative modeling to examine a number of factors which may influence edge shape (notably local ligand symmetry and bond length [13a,c]). Here we consider a simplified model of the typical absorption edge problem, in which we assume a single Gaussian envelope of 1(s) excitations leading to photo-electron release. This has band energy variable, E' , with centre energy E_o and width σ (eV). Typically for Mn, $E_o \sim 6553$ eV and σ is a few eV. We assume only a single class of nearest back scatters, at separation R (eg oxygens at $R \sim 2$ Å). Then the normalized XANES absorption shape, $\mu(E)$ (eg. see a convenient introduction in [ref s1]) is given as a function of X-ray photon energy E , to sufficient approximation for our purposes by;

$$\mu(E) = \frac{1}{\sigma\sqrt{\pi}} \int_0^E \exp[-(E' - E_o)^2 / \sigma^2] \cdot [1 + A_{amp}/k^3 \cdot \sin(2kR + \phi)] \cdot dE' \quad 1)$$

where the photo-emitted electron has wave number k ,

$$k (\text{\AA}^{-1}) = [0.2624 \cdot \Delta E]^{1/2}, \text{ where } \Delta E(\text{eV}) = (E - E'). \quad 2)$$

The term A_{amp} subsumes a number of factors (effective number of ligand back scatters, amplitude reduction term, average ligand scattering amplitude function, Debye-Waller terms, etc.), which depend on the chemical and physical environment (and its variation) of the individual metal (Mn) centres. *All* of these factors (except the scattering amplitude) are likely to compound in *reducing* the effective value of A_{amp} in protein matrices, compared to well ordered model compound systems. For low Z scatters (eg O) with typical metal co-ordination numbers ($\sim 4 - 6$) and bond lengths (~ 2 Å), the effective value of the A_{amp} term is $\sim 1 - 2 (\text{\AA}^{-3})$ and the total k dependence associated with it is given to good approximation by $\sim 1/k^3$, for $\Delta E \sim 1$ eV or more (\sim constant below that [s2]. This is the reason k^3 weighted Mn EXAFS is typically analysed for the photosystem etc.). ϕ is a phase factor, which for mainly low Z scatters in our simplified analysis near the absorption edge (ie low k), we may take as ~ 0 .

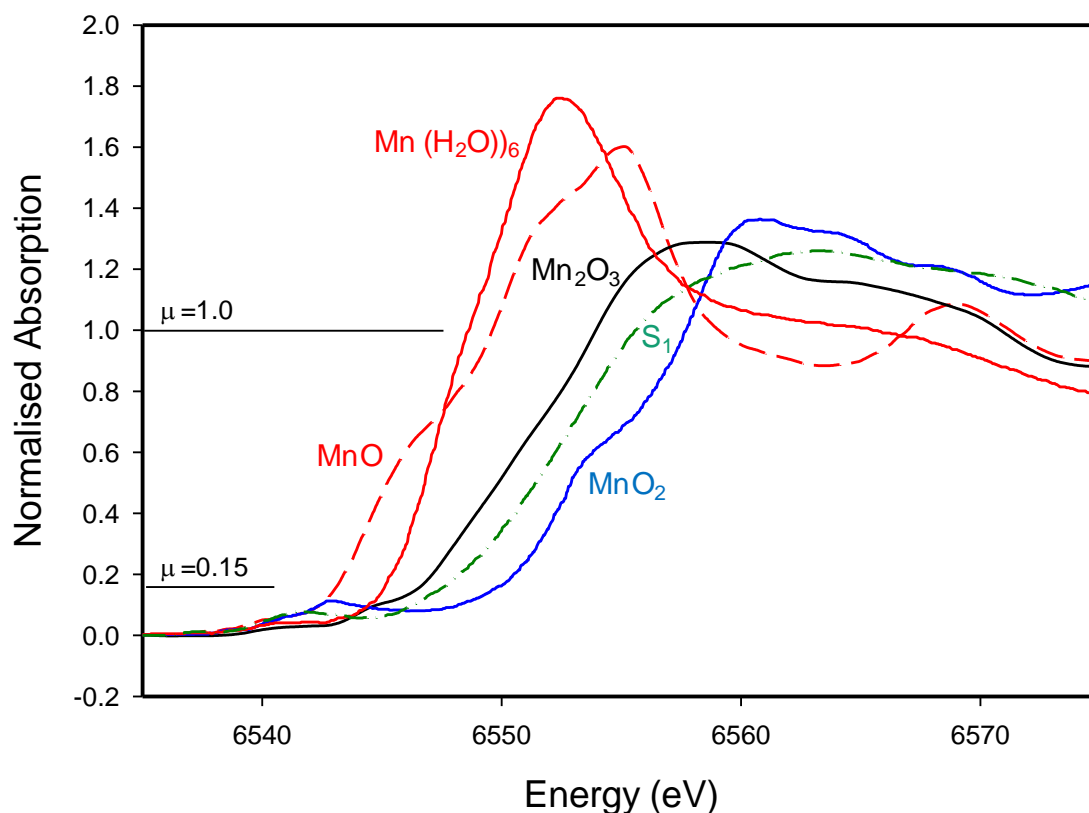


Fig S3a Normalised Mn K edge spectra for Mn reference compounds in Fig 3b, together with S1 spectrum (from Dau et al. [13a]). Absorption limits for integral edge energy determination shown

Fig S3a reproduces the normalised Mn K edge spectra (data from Dau et al. [13a]) for Mn oxides etc., used as reference compounds in Fig 3b (main text), with a typical photosystem S₁ spectrum (other S states not notably different, see [13a]). Also indicated are the normalized limits ($\mu = 0.15$ and 1.0) between which the integral method calculates what is effectively the first moment of the absorption edge energy (E_{Int}). For the case of the two Mn II compounds (MnO and Mn(hexaquo)), the integral method readily accommodates structured or non structured edge shapes, yielding a very similar value for the E_{Int} measure ([13a] and Fig.3). However it is notable is that the photosystem edge has a lower first peak maximum, occurring at higher energy, than any of the reference compounds, including Mn₂O₃, with less resolved detailed structure and overall (EXAFS) modulation. The latter could reflect merely that S₁ has mixed Mn valence states, but the reduced amplitude in the edge region is potentially more significant, since the *total* (back scatter averaged) underlying absorption of the normalized

spectra should be essentially the same in all cases. Thus for the Mn II spectra in particular, intensity is ‘displaced’ from the region above 6560 eV into the edge region (6545-6550). This will clearly have a significant influence on the integrated edge position. Equation 1) reveals the origin of this effect, which is not in fact directly related to the oxidation state *per se*.

Table S1: Model Parameter Values – corresponding Edge Energies

Parameter:	$A_{\text{amp}} (\text{\AA}^{-3})$	σ (eV)	E_{int} (eV)	E_{infl} (eV)	Fig. S3b Curve
	2.0	5.0	6548.9	6550.4	a
	1.2	5.0	6550.1	6550.7	b
	2.0	6.0	6548.5	6549.8	c

$E_0 = 6553$ eV and $R = 2.0$ Å in all cases.

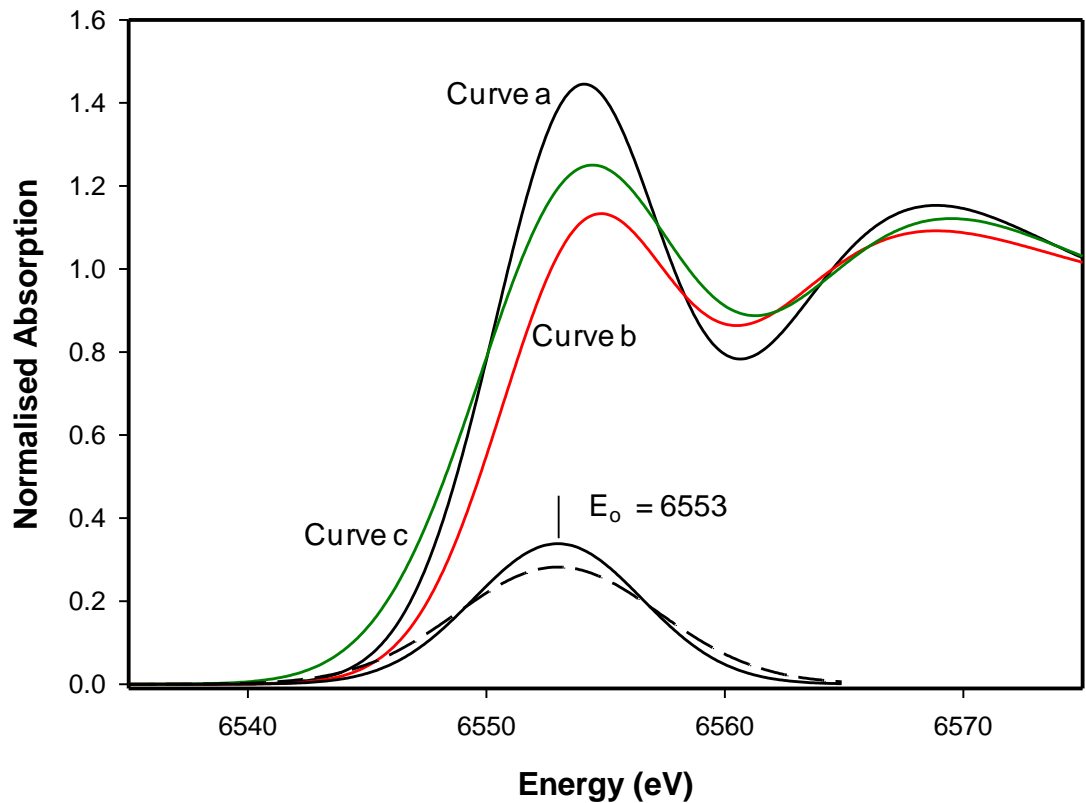


Fig S3b Model Mn K edge absorption profiles, computed using equ. 1), for parameter combinations given in Table S3. Shown also are the $1(s) \rightarrow$ (emission state) transition envelope shapes for the two transition width values, $\sigma = 5$ eV (solid), $\sigma = 6$ eV (dashed).

Fig S3b shows the results of model calculations, using equ. 1), for parameter combinations given in Table S3. Both the computed absorption edge shapes and the assumed $1(s) \rightarrow$ (emission state) transition envelopes are shown. These all have the same E_0 value (6553 eV), corresponding to the same model Mn oxidation state. The computed K region absorption shapes bear obvious, semi-quantitative resemblances to the range of real system data in Fig S3a (remembering that the model data have no relative oxidation state shift, which is ~ 3 eV per equivalent), in particular they exhibit a variation in the 'absorption displacement' and consequent peak shift to higher energy effects mentioned above. The α values and their variation are typical of those seen from detailed TDDFT calculations on a variety of Mn systems [27]. The corresponding inflection point (E_{infl}) and integral edge energy (E_{int}) measures are also indicated in Table S3. Clearly these *all* vary- despite the *formal* oxidation states being the same. For this limited set, the total variation of the integral measure is about twice that of the inflection point measure, notwithstanding the acknowledged utility of the former with structured edges (as noted above). In particular the integral method is at least *three times* as sensitive to variations in the A_{amp} factor, in the limited study here, and this appears broadly true over a range of examples we have examined (not shown). This is very significant because, as mentioned above, it is precisely this parameter, reflecting a number of contributing influences, which is likely to differ most between the calibration set compounds and protein centres. From Table S3, a 40 % reduction in the effective A_{amp} factor causes the integrated edge energy to increase by over 1 eV, with an absorption profile now more closely resembling the OEC shape. The shift is nearly as great as that (~ 1.6 eV) which separates the high and low oxidation state assignments for the OEC in Fig.3b and is in the expected direction :- the apparent OEC oxidation levels are overestimated by comparison with the reference set, particularly at lower oxidation states where the biasing, from Fig S3a is likely to be greatest. It is further notable, from Fig. S3a and the above discussion, that the closest overall qualitative match of the photosystem S1 state edge region shape to the model compounds comes with Mn_2O_3 . This is because Mn III, being a Jahn-Teller ion, has a less regular first co-ordination sphere (and lower number of closest ligands) than Mn in the other oxy species. Precisely the circumstances obtaining in the OEC Mn cluster.

In summary we feel that there are many caveats to be observed in the interpretation of Mn K edge data, with regard to assigning the oxidation states of the OEC. From our earlier TDDFT analyses, factors like the N/O ratio primarily influence the E_0 value in the above illustrative model, and are then inescapable however the edge energy is quantified-unless computationally or otherwise allowed for. The integral method, although clearly attractive from the perspective of objectively averaging over edge structure, may have more fundamental difficulties when comparing systems of different 'local ordering'. Ironically, the inflection point method, employing if necessary multiple inflection point averaging (as in [27]), may be more reliable overall - certainly when combined with computational allowance for what is essentially the E_0 term, as we have shown for a broad range of systems [27, 14].

Supplementary Information References

- s1 Vlaica, G. ; Olivib, L. *Croatica Chem. Acta.* **2004**, 77, 427-433
- s2 McKale, A. G. ; Veal, B. W. ; Paulikas, A. P. ; Chan, S.-K. ; Knapp G. S. *J. Am. Chem. Soc.* **1988**, 110, 3763-3768